Journal of Archaeological Science: Reports 61 (2025) 104939

Contents lists available at ScienceDirect

Journal of Archaeological Science: Reports

journal homepage: www.elsevier.com/locate/jasrep

Multi-scale contact mechanics framework for upper palaeolithic ground stone tools☆

Maria Rosaria Marulli *, Giusi Sorrentino *, Marco Paggi

IMT School for Advanced Studies Lucca, Piazza San Francesco 19, Lucca 55100, Italy

ARTICLE INFO

Keywords:
Ground stone tools
Confocal profilometer
Close-range photogrammetry
Contact mechanics
Boundary element method
Multi-scale analysis
Digital twin model

ABSTRACT

This work presents a multi-scale and multi-resolution digital twin model of Upper Paleolithic ground stone tools (GSTs) to simulate their tribological evolutions. The physics-based digital twin relies on a multi-scale dataset of a passive tool used in a replicative experiment, incorporating the stone macroscale 3D reconstruction and the profilometric microscale surface map. The computational model, simulating a vertical pounding action, allows the prediction of the pressure distributions and the real contact area, where surface modifications due to contact are prone to appear. It is based on the Boundary Elements Method for solving the contact problem at different scales, using the photogrammetric reconstruction of the stone surface at the macroscale and the 3D confocal scanning at the microscale. This unprecedented digital twin model links macroscale to microscale contact mechanics simulations and is validated against experimental replicas, comparing the prediction with the wear patterns observed on the passive tool's surface.

1. Introduction

Archaeological research into artifacts' use-biographies is grounded in the application of functional analysis approaches. When applied to ground stone tools (GSTs), it involves examining their surfaces' traces and wear patterns to gain deeper insights into their functional aspects. By incorporating methodologies such as design analysis, traceology, and particularly use-wear analysis, complemented by residue analysis, researchers can thoroughly evaluate the tools' functionalities and improve their comprehension of artifacts' utilization. It is important to note that functional analysis often relies on establishing a reference collection, a crucial resource for studying the formation processes of diagnostic patterns. This collection acts as a proxy for interpreting and deciphering archaeological evidence (see Adams, 2002; Adams, 2010; Dubreuil et al., 2015; Marreiros et al., 2020, and the literature therein for theoretical discussions and insights into these subjects). The creation of a GSTs reference collection is based on the methodology inherent to experimental archaeology, involving repeated trials of raw material processing with different lithotypes over varying durations, followed by the analysis of wear and, eventually, of residues. Pioneering work by Stemp and Stemp (2001) emphasized the importance of calculating characterization parameters across a range of scales (for an overview of the multi-scale approach, see Brown et al., 2018). Ideally, stone tool topographic analysis relies on a multi-scale approach incorporating multiple techniques such as macroscale 3D reconstruction (using photogrammetry and scanners), application of various microscopes, and, in the last 30 years, quantitative approaches using different profilometer systems to produce microscale surface profiles and maps. In this regard, quantitative methods to digitize GSTs can be extremely useful, and so far, photogrammetry and confocal profilometry have been profitably exploited by the authors (Sorrentino et al., 2023b; Sorrentino et al., 2024). The former can provide 3D models of the whole GSTs. On the other hand, the latter allows scanning much smaller portions of the GSTs surfaces to perform depth analysis of wear traces and surface modifications due to repeated contacts.

Clearly, these approaches are far from being standardized and are highly time-consuming. In this context, experiments involving mechanical setup (Astruc et al., 2003; Calandra et al., 2020; Paixão et al., 2021; Paixão et al., 2022) have provided an initial solution, although they fall short of replicating the flexibility and adaptability of human gestures (see Sorrentino et al., 2023a; Marulli et al., 2023b). In this context, computational mechanics offers new perspectives in realizing digital twin models of GSTs to simulate their tribological evolutions, and attempts to answer some fundamental research questions in a controlled

☆ This article is part of a special issue entitled: '21st Century Traceology' published in Journal of Archaeological Science: Reports.

* Corresponding authors.
E-mail addresses: mariarosaria.marulli@imtlucca.it (M.R. Marulli), sorre.giusi@gmail.com (G. Sorrentino).

https://doi.org/10.1016/j.jasrep.2024.104939
Received 27 July 2024; Received in revised form 8 November 2024; Accepted 16 December 2024
Available online 24 December 2024

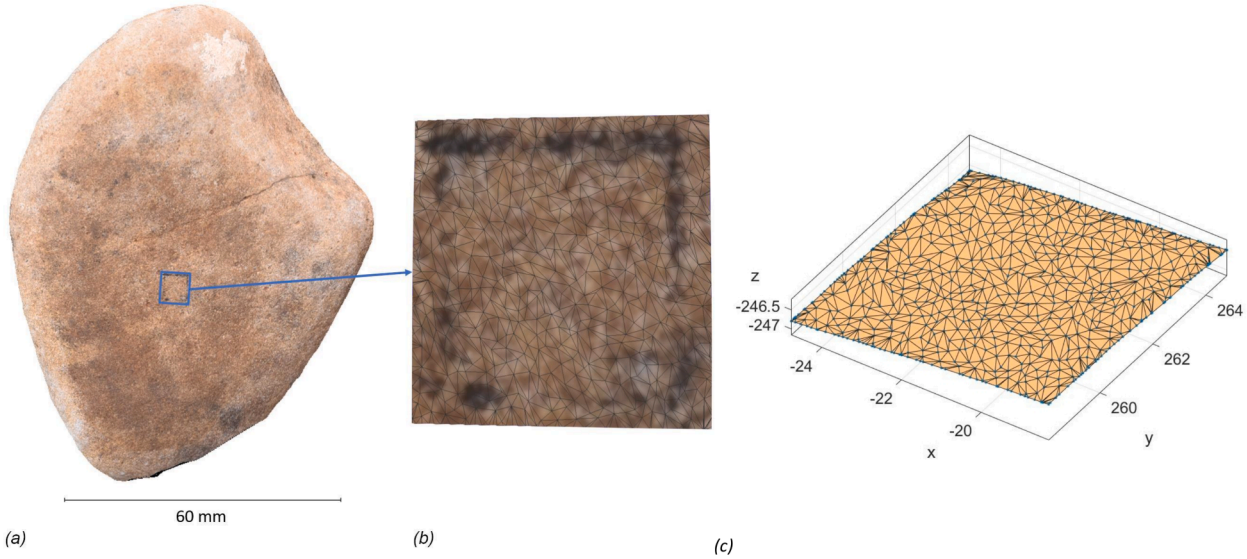

Fig. 1. (a) The quartz-arenite pebble used as a passive tool, referred to as M12 (modified after Sorrentino et al. 2023b), showing the use-surface and the analyzed square highlighted in blue. (b) The area imported for pre-processing in Matlab for the BEM simulation at the macroscale, shown in (c). An area larger than the 5 mm-side square was extracted to have more points for fitting, thereby reducing the error near the square boundaries.

and repetitive environment. Although a complete predictive capability of any computational tool should include all the phenomena responsible for surface fracture and wear formation, also in the presence of a third body in between the lithic tools to mimic with a great deal of accuracy the exact usage of GSTs, a first attempt has been made in (Marulli et al., 2023b) to exploit the 3D photogrammetric model of GSTs to numerically simulate with the Finite Element Method (FEM) the tools' damage and fracture under the action of pounding (percussion loading in the direction perpendicular to the base tool) and of pounding followed by grinding (lateral displacement of a stone with respect to the other, under friction), investigating the effect of human gesture variability on damage patterns.

As shown in (Sorrentino et al., 2024), 3D confocal reconstruction of surfaces, however, provides a great deal of information on local surface phenomena at a scale where frictional effects and wear take place. Although appealing, the use of such data to construct digital twin models of GSTs does present two major challenges: (i) an experimental one, which is related to the difficulty in scanning the whole GSTs using confocal profilometry by stitching individual spot measures and covering at least the whole surface exposed to contact, which is far from being flat; (ii) a computational one, related to the complexity in generating a physics-based digital twin model also considering fine-scale roughness, as attempted in (Marulli et al., 2023a; Bonari et al., 2022) for a limited number of model surfaces.

In this work, we propose an unprecedented multi-scale computational framework in the field of contact mechanics to overcome the above challenges and link macroscale to microscale contact mechanics simulations based on the so-called Boundary Element Method (BEM). The methodology will also make use of different geometrical data in input, creating a theoretical framework to link contact problems at the tool macroscale, using 3D photogrammetric reconstructions, and contact problems at the microscale where wear builds up, using 3D confocal geometries. This overcomes the limitations of photogrammetry in terms of limited surface resolutions and of confocal profilometry in terms of maximum sampled lateral size. It will be shown that the proposed digital twin model of GSTs can be exploited to predict the real contact areas and the regions where use-wear traces are more likely to develop at different scales, also considering the mechanical property of the lithic material involved.

A previous attempt to simulate wear trace development on lithic tools using methodologies coming from a different research field was conducted in (Rausch et al., 2024), where occlusal fingerprint analysis (OFA), a well-established method in dental wear studies, was employed to identify the location of sequential contact points between opposing surfaces. With the same spirit of crossing the disciplines, as already attempted in (Marulli et al., 2023b), the present contribution exploits methodologies coming from the computational mechanics community, where the physics beyond friction, wear, and surface damage phenomena are deeply studied for designing surfaces in relative motion (for example bearings, wheels, coatings, etc.) for GSTs use-traces analysis.

This work is the first step for the validation of a multi-scale BEM-based digital twin model for the simulation of GSTs use-wear traces and opens to many possible applications in the field of lithic functional analysis as a supporting tool for experiments and for simulated tests on the archaeological records. As detailed in the following, the developed digital twin simulates the contact interaction between a passive stone tool and a hypothetical flat surface assumed as the active tool. The simulation considers both the macroscopic level and the microscale, employing the photogrammetric data and the confocal profilometric acquisition of the passive tool's use surface. Section 2 details the surface documentation procedure, the methodology for integrating the two scales, and the development of the physics-based digital twin model based on the BEM algorithm. The simulation results are presented in Section 3 in terms of predicted contact areas and contact pressure distributions for the two scales of investigation. They are compared with experimental wear patterns to validate the methodology. Section 4 draws the conclusion and discusses possible extensions of the proposed methodology to more complex scenarios, including the possibility of analyzing the contact interactions of two ground stone tools, simulating grinding and pounding actions, and, in general, employing BEM for use-wear localization and quantification in archeological studies. This method has the advantage of being completely non-invasive and requires a minimum interaction with the stone tools, implying its applicability also to archaeological artifacts once the methodology is validated on experimental tools.

2. Material and methods

This article specifically focuses on a quartz-arenite pebble, referred to as M12, collected from the Racovăț river banks (Moldova) and used as a passive tool in a replicative experiment of plant processing (Fig. 1a). M12 has an irregular shape, with a slightly concave profile of the used

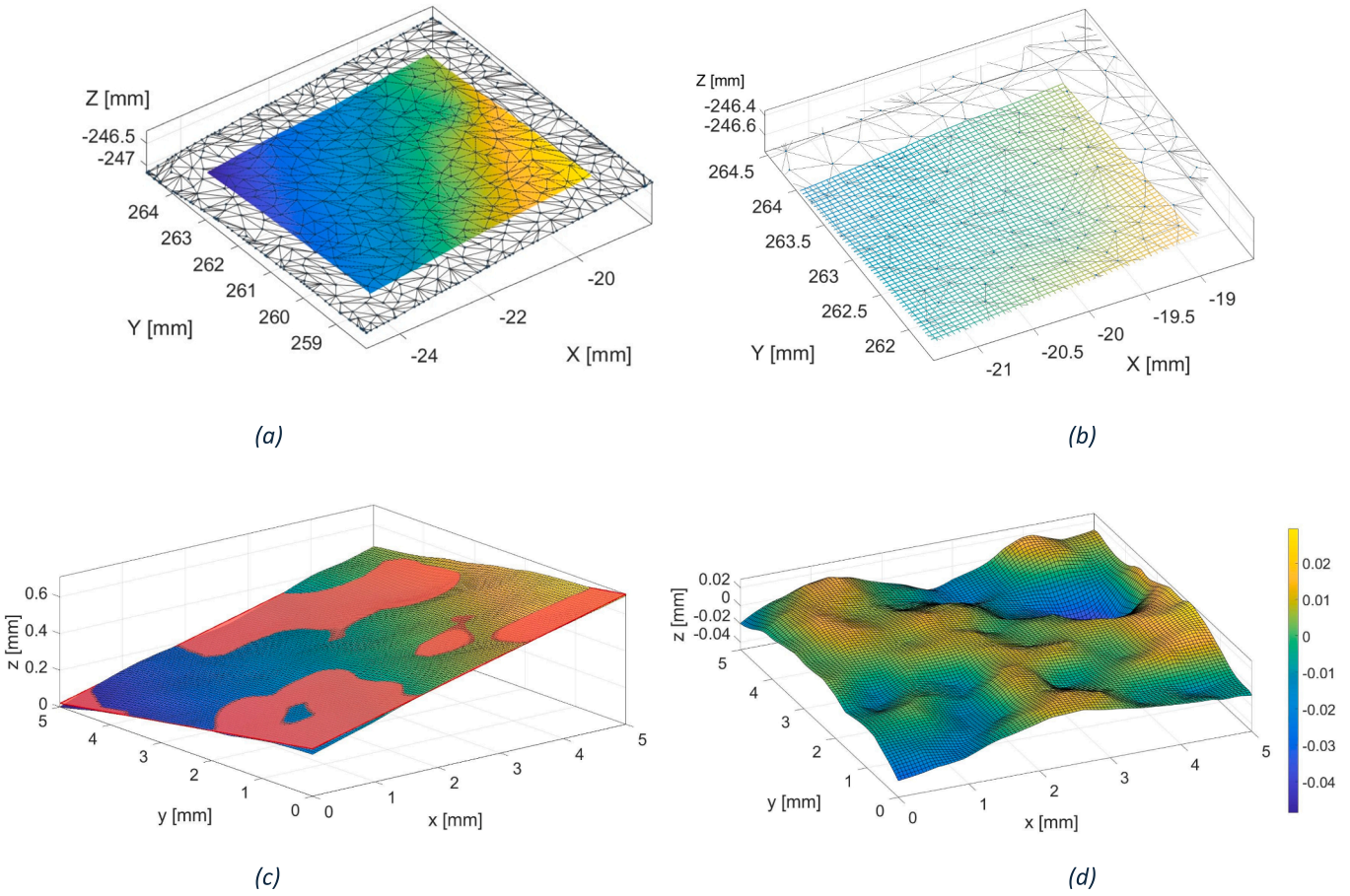

Fig. 2. (a) Regular grid interpolated to the stl points cloud and extraction of the 5 mm-side square area (b) Magnification of a small area of the previous plot showing the regular grid of boundary elements. (c) Plane interpolated to the stone surface to remove its inclination; (d) stone surface after removing the interpolated plane.

surface, a length of 100.38 mm, a width of 80.57 mm, and a thickness of 29.5 mm (Sorrentino et al., 2023b). The used surface was documented before the experiment (T0) and after 30 min of use (T1). The strategy included a multi-scale approach to experimentally document and analyze the tool's geometry and surface, as (Sorrentino et al., 2023a) reported. This involved 3D model reconstruction through close-range photogrammetry (as reported in Sorrentino et al., 2023b) and roughness surface documentation and quantification via confocal profilometer scanning of a selected region of 5x5 mm at the center of the use-surface (as reported in Sorrentino et al., 2024).

Given that surface interactions occur across multiple scales of surface topography, a systematic approach should integrate a multi-scale analytical strategy. The combination of digital 3D data collected from photogrammetry and confocal profilometry at T0 enables the simulation of contact stress on the passive tool considering contact with a hypothetical active flat horizontal surface. Integrating the two scales allows identifying real contact areas at multiple scales of analysis and calculating possible regions more susceptible to mechanical stress where wear is likely to develop. Finally, this methodology is validated by comparing the simulated data with the real data acquired on M12 at T1.

Macroscale topographies acquired using photogrammetry can be passed in input to computational mechanics software to simulate and predict the overall force–displacement relation induced by the normal contact of two GSTs during pounding. In this regard, two modeling options could be invoked: the finite element method as in (Marulli et al., 2023b) or the boundary element method as proposed in the present study.

The FEM is based on the discretization of the volume of the analyzed solids in small units called "finite elements" in order to solve numerically the equations describing the solids' deformation caused by applied mechanical loads, as well as their interactions. This method allows to compute the displacement and force distributions within the solids, as well as other mechanical phenomena such as damage and fracture at each node of the solid mesh. In some applications, as in the context of contact problems between rough surfaces, the FEM simulations can be computationally expensive, especially when the problem is treated at the microscopic level due to the high number of nodes required for accurately representing the surface roughness and the solid volume. In these cases, a BEM formulation can be more efficient since the underlying mathematical formulation allows to discretize only the surface, using small quadrilateral elements called "boundary elements" to compute the surface displacements and force distribution caused by the contact interaction, while the state of the volume can be obtained with a post-process operation if needed (Vakis et al., 2018, Müser et al., 2017).

This approach is particularly suitable for the present application, where we focused on the analysis of a portion of the passive stone tool's surface whose size is smaller than the whole tool size, a condition necessary for the application of the BEM, where the solid is considered to be of infinite size (see Liu et al., 1999; Bemporad and Paggi, 2015; Rey et al., 2017 for the fundamentals of the mathematical method and its algorithmic implementation). Applying BEM for contact problems allows to simulate what happens when the tool surface comes into contact with a hypothetical flat surface. The BEM algorithm requires in input the mechanical properties of the solids and the surface topography, and quantifies the surface deformation and the force distribution on the surface at each boundary element, together with the contact areas and

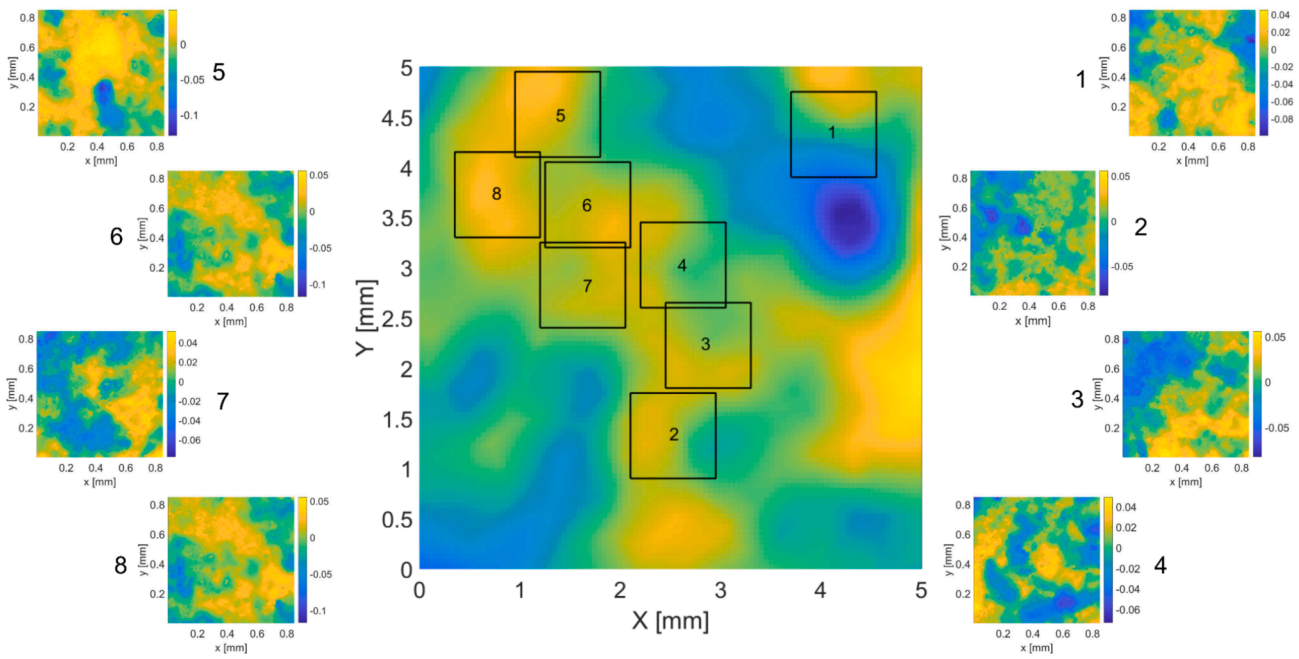

Fig. 3. View of the multi-scale acquisition showing the microscale rough surfaces' location on the macroscale topography.

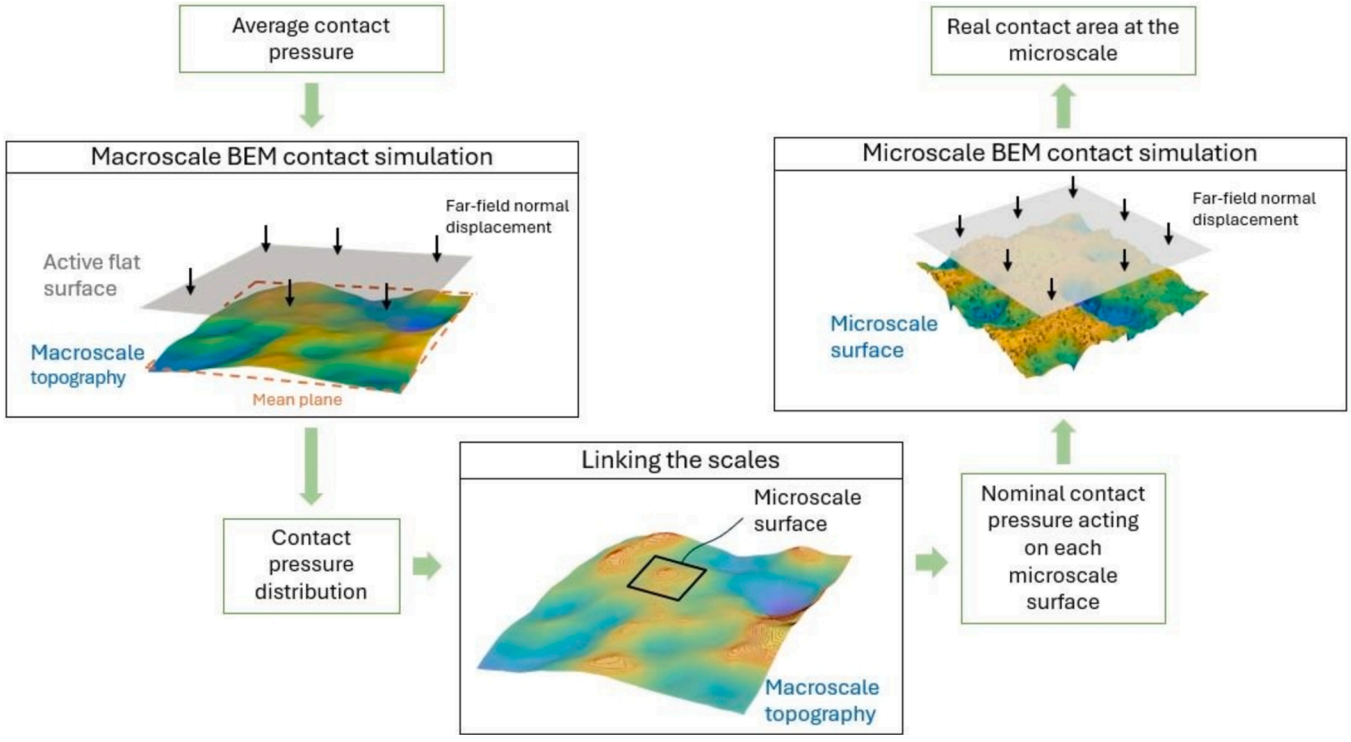

Fig. 4. Multi-scale contact mechanics framework.

the overall force–displacement relation induced by the normal contact. Compared to the FEM approach in (Marulli et al., 2023b) where the GSTs have been modeled at the macroscale using photogrammetric data, in this work, the BEM is employed to represent with great accuracy the surface of the GST exploiting photogrammetric and profilometric data, with the aim of predicting the portion of the tool surface that will develop wear traces. In fact, according to theoretical arguments in contact mechanics (Ciavarella, 1998; Jäger, 1998; Hills and Moore, 2022), the contact areas found solving the normal contact problem are the areas where repeated grinding operations may cause wear and fretting fatigue due to microslip displacements.

The multi-scale (multi-resolution) approach proposed in this study solves the contact problem at two scales. The first step consists of the simulation of the contact problem at the macroscale using the photogrammetric surface (acquired as outlined in Sec 2.1) to compute the average nominal normal pressure acting on each microscale surface acquired using confocal profilometry, as described in Sec. 2.2. In the second step, the computed nominal average pressures (here, the loads

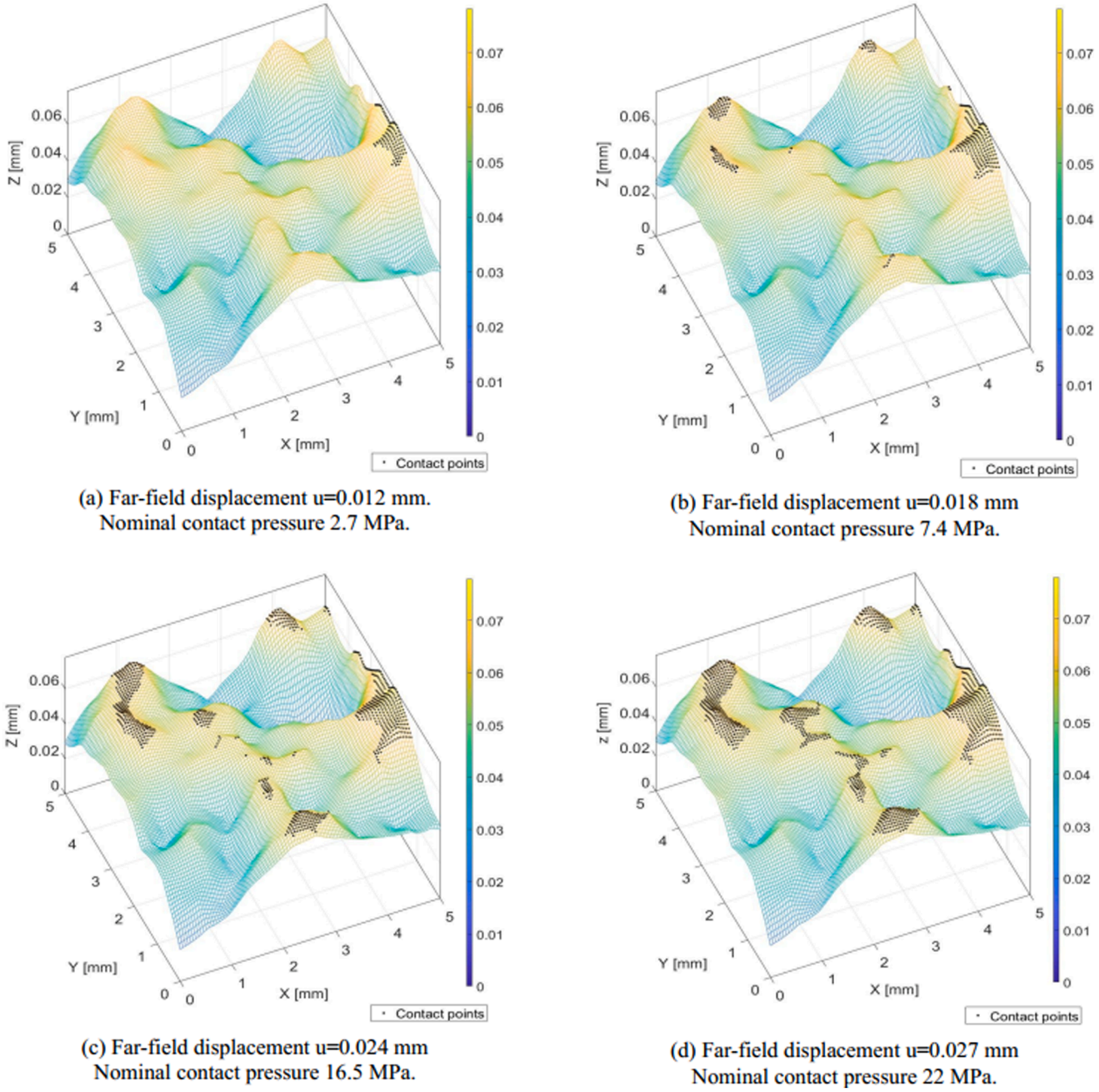

Fig. 5. BEM simulation of the macroscale topography for an increasing value of the applied far-field displacement in the direction normal to the mean surface plane: black spots refer to boundary elements in contact.

are scale-invariant quantities, see Carpinteri and Paggi, 2005) are used for the simulation of the contact problem at the microscale, linking the two scales according to the method described in Sec 2.3. Details on the multi-scale computational framework implementation are given in Sec 2.4.

2.1. Photogrammetric data

The photogrammetric acquisition was performed to reconstruct the geometric characteristics of the artifact. Structure-from-Motion (SfM) and Multi-View Stereo (MVS) techniques were used to create detailed 3D models of the GST before and after the experimental tests. A custom setup was designed and thoroughly documented in (Sorrentino et al., 2023b) to ensure precise and repeatable positioning of the samples. After each use in the experimental simulations, the artifact was consistently repositioned in the same orientation within the setup to maintain accuracy. A total of about 114 images per object each time were processed using Agisoft Metashape software, and the resulting model mesh was exported in STL format. The M12 STL file was then cut to extract the area measured by the confocal profilometer (Fig. 1), corresponding to the 5 mm-side black square marked on the surface. The mesh had an average edge length of 0.3144 mm.

The BEM requires a surface discretization made of a regular mesh of square elements. Therefore, the STL surface triangularization, shown in Fig. 1b, must be pre-processed to create a suitable regular mesh. The file has been imported in MATLAB R2024a using the function “stlread” from (Doron, 2024) (see Fig. 1c). The points cloud has been fitted by a regular grid composed of 100x100 square elements using the built-in MATLAB function “scatteredInterpolant” (Amidror, 2002) as shown in Fig. 2. To reduce the error of the fitting procedure near the boundaries, the STL

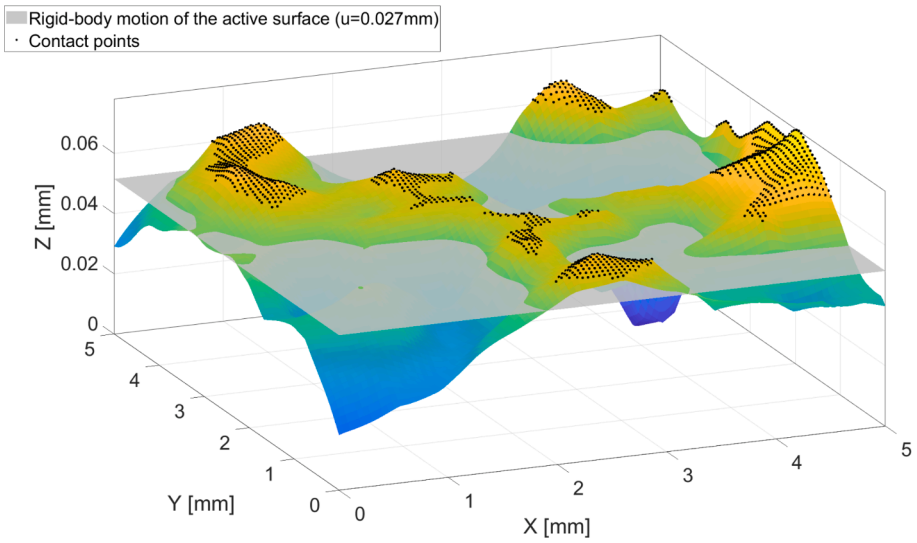

Fig. 6. The contact areas computed by the BEM algorithm (black dots) represent only a subset of the areas that would result in contact considering a rigid compenetration of the active surface, neglecting the active surface elastic deformation. The plot represents the simulation results for a far-field displacement u = 0.027 mm and a nominal contact pressure of 22 MPa.

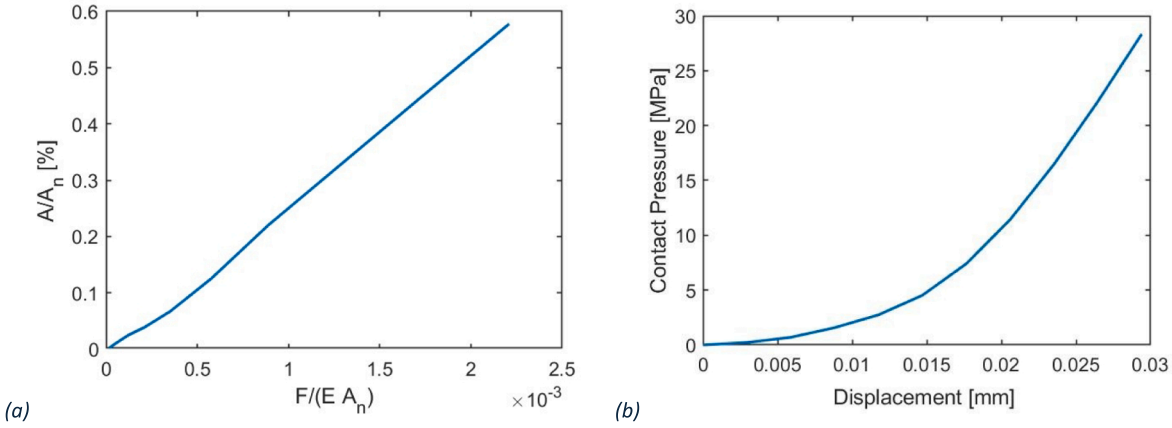

Fig. 7. (a) Percentage of the real contact area A/A_n vs the adimensional contact force $F/(E\ A_n)$; (b) nominal contact pressure vs. far-field displacement.

point cloud consisted in an area bigger than the 5 mm-side square, as shown in Figs. 1 and 2, and the target square has been extracted only after the interpolation.

Another step of the macroscale topography preparation consisted of the removal of the geometric characteristic of the tool, subtracting to the selected square the surface inclination by fitting a plane and subtracting it from the surface topography map, see Fig. 2c. The final result of the pre-processing phase is shown in Fig. 2d.

The selection of a square in a nominally flat area situated in the center of the working surface, away from the curvature of the stone edges, allows to consider negligible the effect of the detrending of the surface on the results of the contact problem since the hypothetical active surface considered in the BEM is taken parallel to the mean plane of the passive surface. This operation has been performed in order to have a homogeneous treatment with respect to the microscale where the detrending operation is necessary to remove possible artifacts induced by the mold used for the profilometric acquisition, as explained in the following section.

2.2. Confocal profilometric data

The Leica DCM 3D dual-core measuring microscope in confocal mode was used to acquire microtopographic maps of the selected square. To ensure permanent documentation of the square, polyvinyl siloxane molds were used to create a physical negative copy of the surface, following the strategy outlined in (Sorrentino et al., 2024). The copied square on the mold was scanned using the 10x lens in 25 areas of 0.85 x 0.85 mm and 512 x 512 data points each (corresponding to a sampling interval of 1.66 μm).

The scanning was performed at T0, before tool utilization, and at T1, after 30 min of use, to compare the scanned areas and verify modifications due to use. Because the drawn reference square was less visible after use, there was no exact overlap of the 25 areas scanned at T0 and T1. However, since the analysis was supported by imaging data coming from the confocal microscopy option given by the Leica instrument, a visual comparison with the acquired point was also used as cross-check for the overlapping of the two times. Therefore, in the present study, we consider only the areas where the overlap is more precise. Additionally, when positioning the microscale topographies onto the 3D model as described in Sec. 2.3, it was noted that some of the microtopographies were located in areas where the contact with a hypothetical flat active tool surface at the macroscale does not occur (neglecting the medium in this simulation). Consequently, these areas were excluded from the analysis.

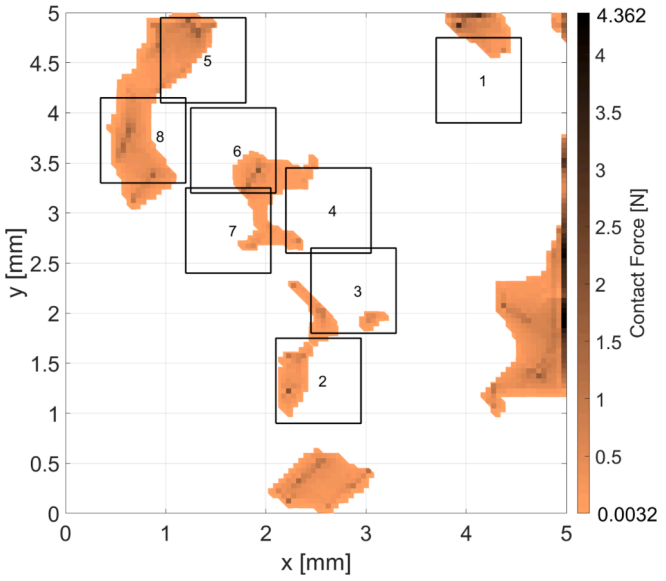

Fig. 8. Contact force distribution on the macroscale surface for a far-field displacement u = 0.027 mm, and location of the microscale surfaces.

Table 1
Average pressures computed from the BEM solution of the contact problem on the macroscale topography, passed in input to the microscale BEM simulations.

Microscale surface	Nominal pressure [MPa]
1	8.07
2	22.77
3	11.92
4	4.83
5	71.08
6	25.71
7	11.17
8	76.07

As the molds represent the negative copies of the surfaces, data acquired on them were inverted on the z-axis and flipped along the x-axis before analysis to simulate conditions on the actual tool surface. In terms of post-processing of the raw sample topography, a few points over the surface were clearly wrongly detected since they constituted evident outliers far from the other surrounding elevations. However, instead of relying on a specialised commercial software as e.g. (Calandra, 2022) or manually replacing the elevation of such points, an automatic algorithm has been implemented in MATLAB R2024a, (available as supplementary material). The procedure scans all the surface elevations (i,j), with i,j = 1,…,512, and computes the threshold values $z_{ave} \pm k\sigma$, where z_{ave} and σ are the average and the root mean square of the heights of the points within a squared area of lateral size ± r centered in (i,j). The coefficient k is identified by the algorithm using a bisection method in order to replace a user-defined maximum percentage of surface elevations. In the present study, excellent results have been obtained with a percentage of 1 %.

Moreover, the microscale topographies have been prepared for the analysis by removing the surface inclination following the procedure described in Sec.2.1 for the macroscale since the non-zero slope could be an artifact induced by the limited size and the non-perfectly planar backside of the polymeric molds used to acquire microtopographic maps, which may have irregular borders or irregularities outside the physical geometry of the stone.

2.3. Linking macroscale (photogrammetry) topographies to microscale (confocal) surfaces

As described above, the multi-scale framework proposed in this work is based on coupling the fine-scale roughness data obtained from the confocal profilometer onto the geometry and waviness acquired from the photogrammetric 3D documentation. During the confocal profilometric acquisition, this task has been accomplished using a single reference point as the origin of a global reference system corresponding to the top-right edge of the square area, and reconstructing the location of the microscale surfaces at time T0 through their x and y coordinates.

The reference point, visible also at the macroscale in the 3D model, has been exploited for the positioning on the xy plane of the microscale surfaces on the photogrammetric acquisition, as depicted in Fig. 3, while the detranding operation compensates for the spatial tilting allowing their placement also on the z.

This procedure, even though not exact, allowed linking the scales with reasonable accuracy. Moreover, it has been verified by checking manually that some peaks and valleys visible at the macroscale correspond to the waviness of the microscale surfaces. An optimization of this task could be implemented using a different technique to mark the reference point at the two scales with better accuracy, especially for increasing the visibility of the reference square after use. However, this is beyond the scope of this work and is left for future research.

2.4. Proposed multi-scale contact model

The BEM algorithm solves the contact problem between the passive stone surface (rigid rough surface) and a deformable flat surface of a hypothetical active tool parallel to the mean plane of the passive surface. The input data BEM requires are the active surface topography and the mechanical properties of the contacting solids.

The displacement applied to the active surface to come in contact with the passive surface is called “far-field displacement”. Due to the roughness/waviness of the tool’s surface, the areas in contact for a given value of far-field displacement would be a certain percentage of the total surface area. The BEM method employs an iterative procedure to identify the areas in contact, assuming as a first trial that the active surface moves as a rigid body and the contact areas are represented by the areas where there is a compenetration between the two surfaces. In reality, there is no compenetration, and the contact areas are only a subset of the ones selected in the first trial because of the active surface elastic deformation. Moreover, the algorithm quantifies the value of the contact pressure that the two surfaces exchange at the contact points.

The simulation results strongly depend on the mechanical properties assigned to the contact surfaces, consisting of the elastic modulus and the Poisson ratio provided in input. The mechanical properties of the quartz-arenite pebble to be used in the contact simulations were not available in the literature; hence, the elastic modulus and the Poisson ratio have been assumed equal to 19.5 GPa and 0.24, respectively, as done in (Marulli et al., 2023b). The elastic modulus value is not used directly in the BEM algorithm, but it is employed to compute the so-called “equivalent” or “composite elastic modulus” according to mathematical equivalence demonstrated in (Barber, 2003), in order to simulate the case of two stone tools in contact, and not the case of one deformable stone against a rigid one. The equivalent elastic modulus is: $E^*=[(1-\nu_1)/E_1 + (1-\nu_2)/E_2]^{-1} = 12.82\ GPa$ with $E_1 = E_2 = 19.5\ GPa$ and $\nu_1 = \nu_2 = 0.24$, supposing that the two stones have the same material properties.

The analysis is performed at two scales, first solving the problem at the macroscale using the photogrammetric topography pre-processed as detailed in Sec. 2.1, and then repeating the BEM simulations at the microscale exploiting the macroscale results. The multi-scale (multi-resolution) computational framework is schematically represented in Fig. 4.

As previously said, the macroscale contact simulations performed

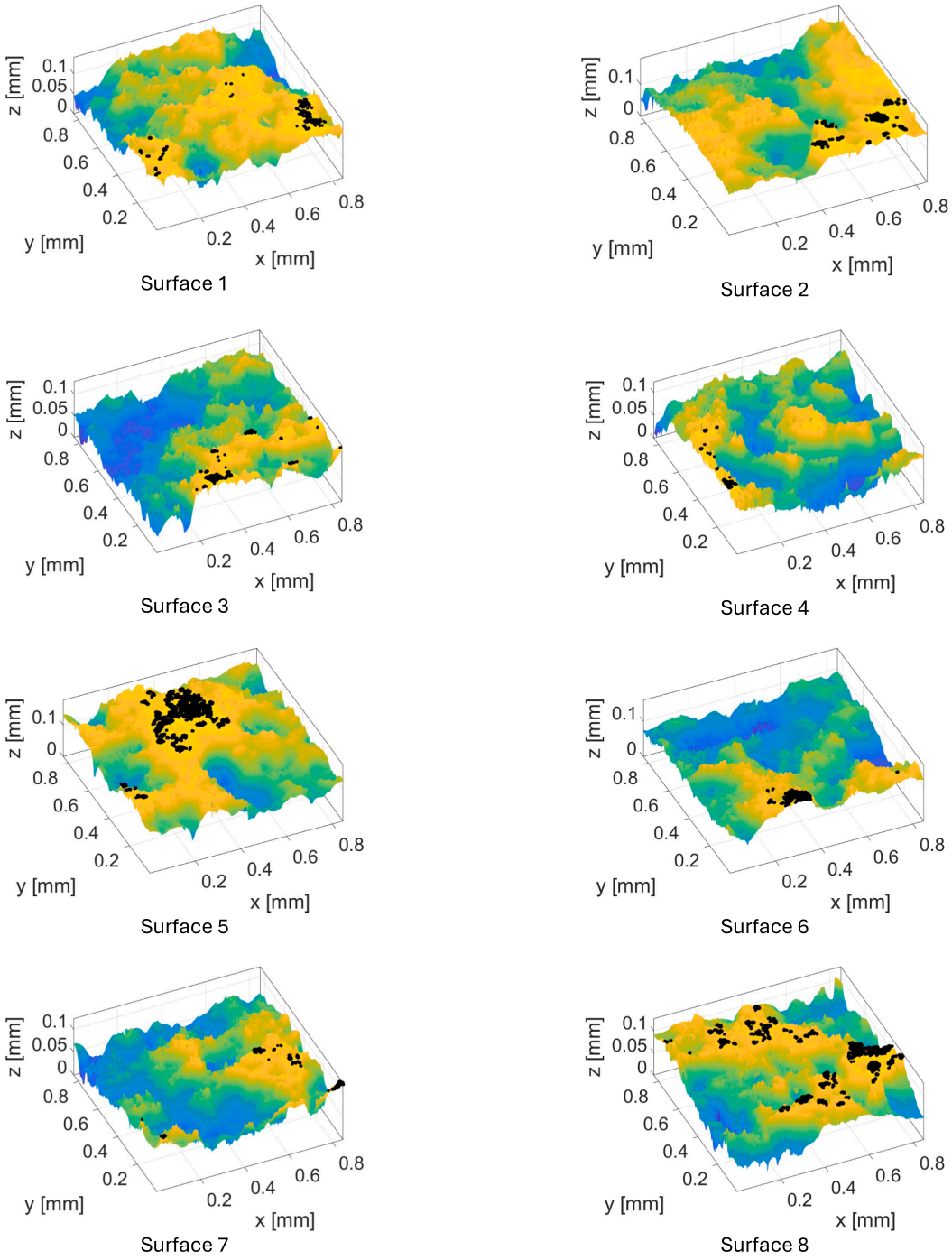

Fig. 9. Microscale surface topographies with contact areas in black as predicted by microscale BEM simulations.

according to BEM provide the corresponding boundary elements in contact and the respective nominal contact pressures (forces divided by the nominal area of the patch) for each far-field imposed displacement. The integral of the contact pressures over all the elements in contact at the macroscale leads to the normal contact force F, which, divided by the nominal contact area ($A_n = 25$ mm^2), provides the average contact pressure that can be compared with the same value measured in the experiments or obtained from other computational simulations that replicate the whole action of pounding between the GSTs.

In the present case, the FEM digital twin model in (Marulli et al., 2023b) predicted an average contact pressure during pounding between similar GSTs of about 22 MPa (corresponding to a normal force of 250 N acting over a nominal contact area of about 11 mm^2). This value is considered as the maximum pressure to be reached in the present BEM macroscale simulations.

Once the macroscale contact problem related to the macroscale topography has been solved using BEM, the multi-scale (multi-resolution) approach is invoked to solve the normal contact problem of the microscale surfaces acquired using confocal profilometry and located over the macroscopical surface.

The information to pass from the macroscale problem to the microscale one is the nominal pressure acting on each microscopical surface within the macroscale model. At this scope, the contact forces exerted onto the boundary elements in contact in the macroscale model that fall within the area of influence of each microscale surface are summed up and divided by the corresponding microscale surface's nominal area

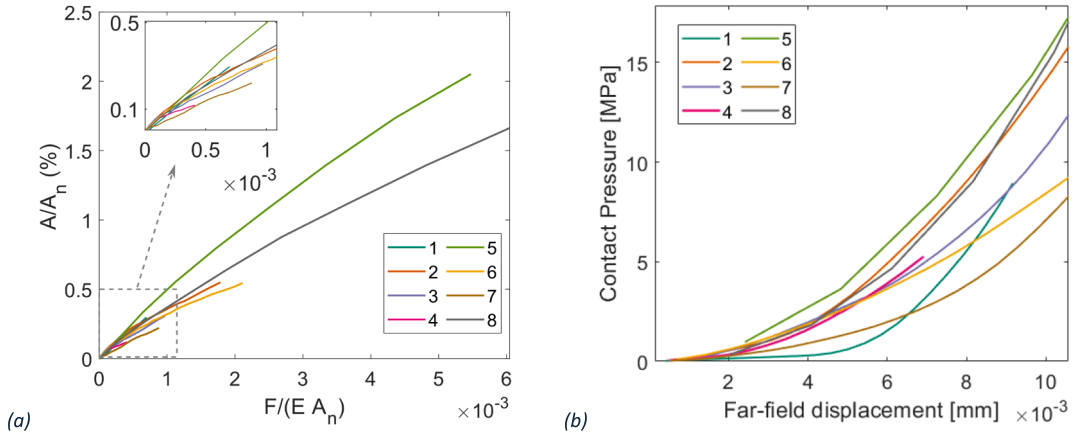

Fig. 10. (a) Real contact area percentage vs. dimensionless normal contact force, (b) nominal contact pressure vs. far-field displacement for each microscale surface whose contact has been simulated using BEM.

(0.7225 mm^2). This measure gives the nominal pressures acting on each microscale surface, which differs from surface to surface. Based on such data, microscale BEM contact simulations are carried out with the microscale rough surfaces obtained by confocal profilometry used in input for the contact algorithm, and by imposing an increasing value of the far-field normal displacement up to reaching the nominal pressure given by the macroscale computation for that considered surface. Once that pressure level is reached, the microscale contact simulation is stopped and a refined analysis of the predicted contact domain is made.

3. Results and discussion

This section presents the results of the multi-scale simulations conducted on the passive tool M12.

As described above, the macroscale BEM simulations have been conducted increasing the imposed far-field displacement up to the target average contact pressure of 22 MPa. The evolution of the contact areas is depicted in Fig. 5, where black dots mark the boundary elements in contact.

For a given value of the far-field displacement applied to the flat active surface, the BEM algorithm computes the contact areas considering the elastic deformation of the active surface. In fact, the obtained contact areas do not simply correspond to the areas having an elevation bigger than a certain value (as in the case of a rigid compenetration of the active surface into the rough passive surface), but they depend on the mechanical properties of the active surface, as explained in Sec. 2.4. This fundamental aspect of BEM is visually explained in Fig. 6 where the nominal contact pressure reaches the target value of 22 MPa for an applied displacement of 0.027 mm. The contact areas obtained with BEM represent a subset of the areas that would result in contact considering only the rigid motion of the active surface.

Moreover, the macroscale contact simulation gives the percentage of the real contact area A with respect to the nominal contact area A_n, that can be related to the dimensionless normal force F divided by the elastic modulus and the nominal contact area, see Fig. 7a. The plot in Fig. 7b also shows the evolution of the macroscale nominal contact pressure, F/A_n, vs. the far-field displacement applied to the active flat surface.

The location of the eight representative microscale surfaces, whose topography has been acquired using the Leica DCM3D confocal profilometer, is shown in Fig. 8 over the contact forces distribution computed by the macroscale BEM simulation, where a value of the contact force greater than zero implies that the point is in contact.

For each microscale surface, the scale-invariant quantity transferred from the macroscale to the microscale is the contact forces acting on the area of influence of the considered microscale surface, divided by its nominal area. In fact, the contact force is the same at the two scales of observation, see the theoretical considerations based on renormalization group theory applied to contact mechanics in (Carpinteri and Paggi, 2005).

The computed average pressures from the macroscale BEM simulations are collected in Table 1 for the eight examined surfaces. They range from low pressures of about 4 – 8 MPa (surfaces 4 and 1) to high pressures between 71 and 76 MPa (surfaces 5 and 8). Those pressures are passed in input to the microscale BEM contact simulations carried out under displacement control until the same contact pressure is attained. The microscale analyses allow a closer examination of their mechanical response, with a higher resolution of the surface map given by the confocal profilometer.

The BEM predictions of the contact mechanics simulations carried out on the eight microscale topographies are shown in Fig. 9, where the boundary elements in contact at the end of the simulation for the maximum attained average pressure are highlighted in black.

The microscale results are also shown in Fig. 10 in terms of the evolution of the real contact area percentage vs dimensionless average pressure (Fig. 10a) and in terms of contact pressure vs far-field imposed displacement (Fig. 10b).

Apart from some scatter induced by the randomness of the microtopography map, all the surfaces present almost the same trend between real contact area and dimensionless pressure, with different extents on the maximum real contact area depending on the surface morphological features.

These results are essential from the physico-mechanical viewpoint for two reasons. First, the amount of predicted real contact area at the end of the contact mechanics simulations provides a quantitative indication of the area of the GSTs in contact which perfectly adheres under the action of a pure normal force. A subsequent application of a shearing loading to the stones, as may occur during the grinding operation with GSTs, would lead to a progressive evolution of the contact domain from *full stick* (no relative tangential displacements between the GSTs) to *full slip* conditions (full sliding between the GSTs), followed by gross sliding. The dynamics of the stick–slip transition can be quantified from BEM contact predictions by exploiting the Cattaneo-Mindlin analogy, theoretically established by Ciavarella (1998) and Jäger (1998) and computationally generalized to rough surfaces in (Borri-Brunetto et al., 2001; Paggi et al., 2014). As well-established in tribology, the contact area subject to such a shearing relative motion would be prone to wear and, in case of repeated loading, fretting fatigue with sub-surface cracks propagating cycle by cycle may also occur (Hills and Moore, 2022). In this regard, numerical results in Fig. 8a shows that surfaces 5 and 8 are those expecting the largest portion subject to wear or fracture. Second,

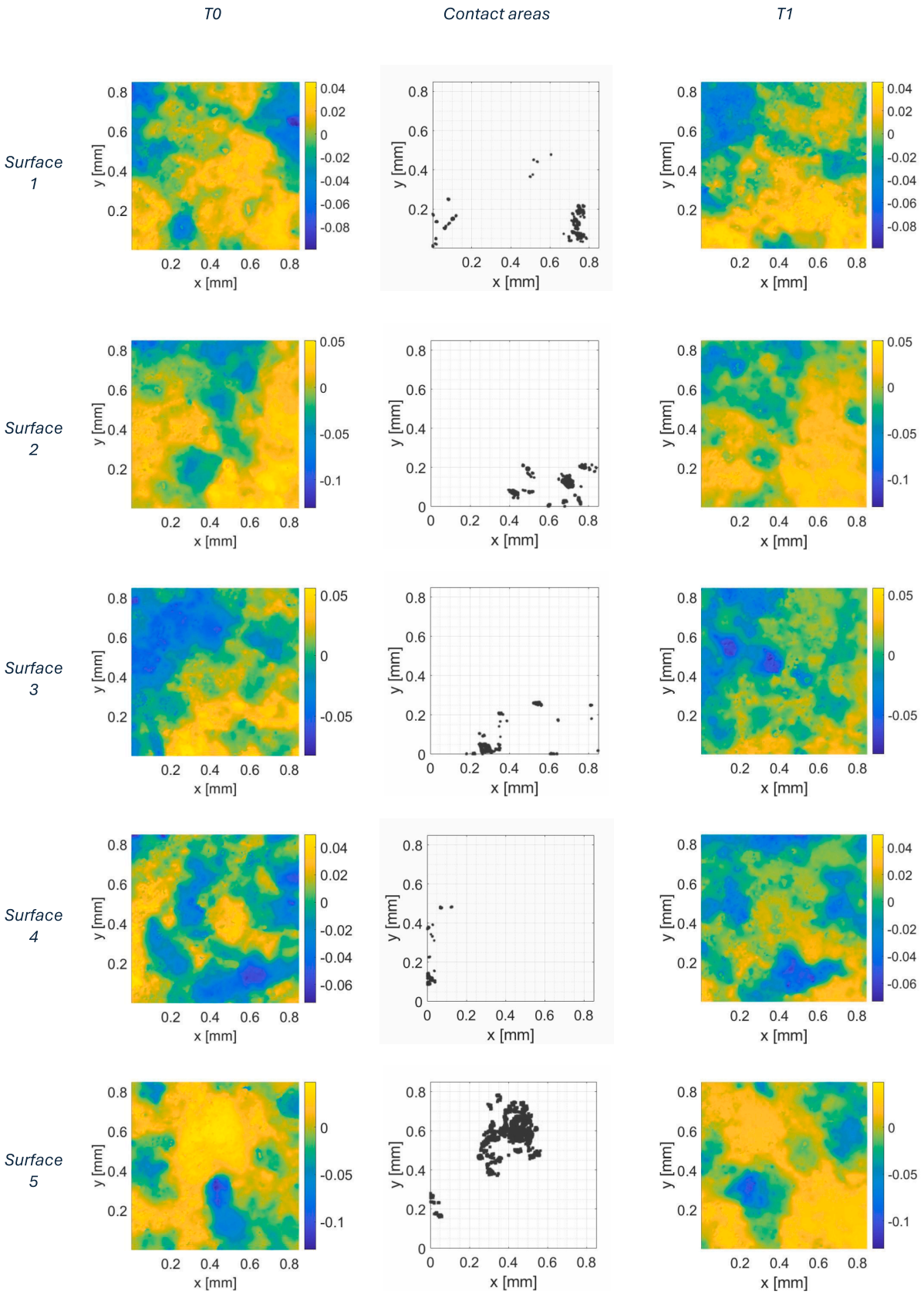
T0
Contact areas
T1
Surface 1
Surface 2
Surface 3
Surface 4
Surface 5
x [mm]
y [mm]

Fig. 11. Acquired microscale surfaces at time 0 (first column) and the areas in contact predicted by the numerical framework (second column) compared to the surfaces at time 1 (third column).

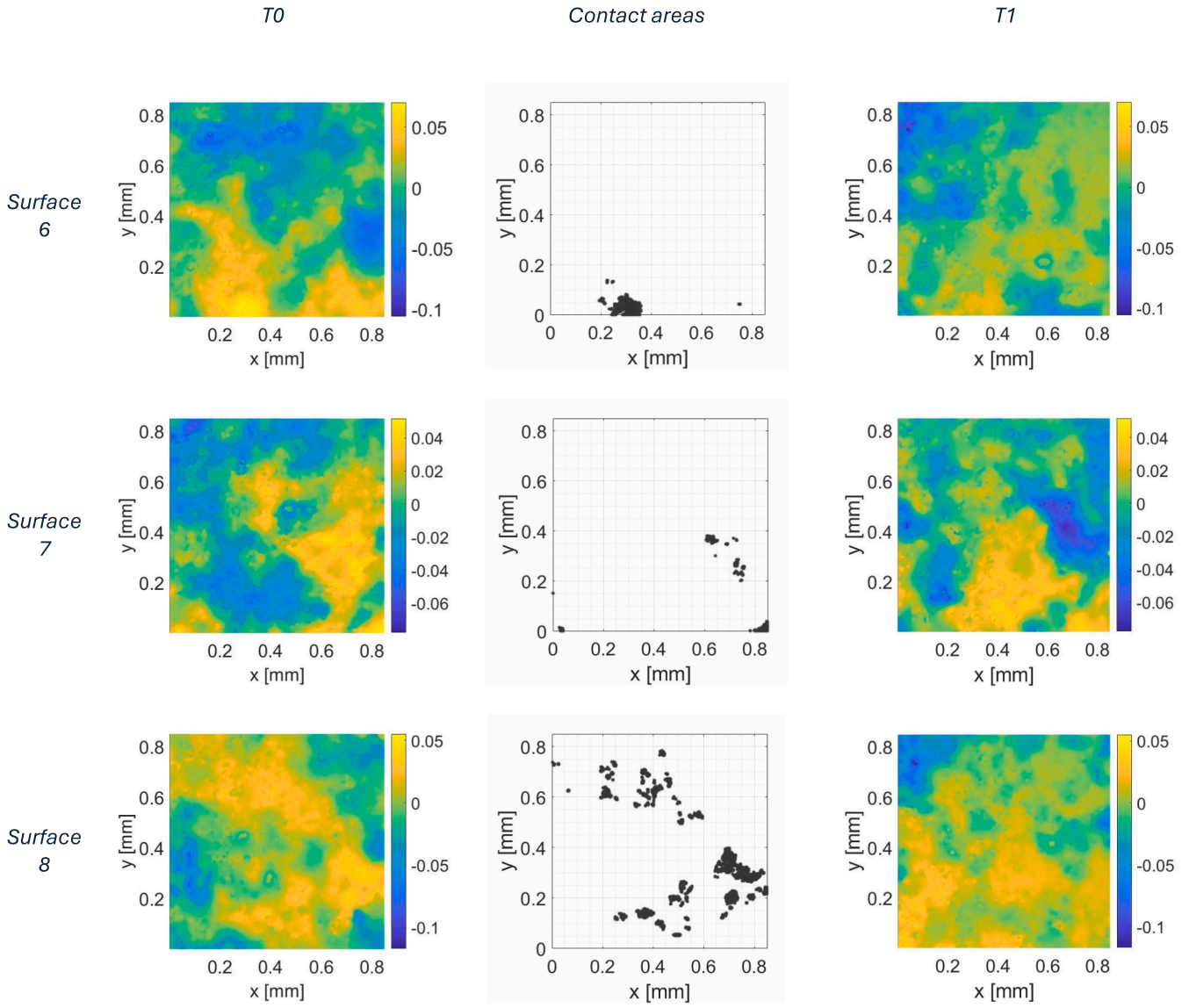

Fig. 11. (*continued*).

the derivative of the contact pressure–displacement relation provides the normal contact stiffness.

From BEM simulations, the majority of GST microsurfaces have a similar contact stiffness evolution, and only three surfaces (1, 6, and 7) are slightly more compliant (low stiffness) during contact. This might affect the tools' ability to crush seeds and other materials interposed in between, with the major pounding effect in the locations where the stiffness is higher.

In this regard, Fig. 11 presents a comparison between: (i) the microscale surface topography acquired at time 0; (ii) the real contact areas predicted by the BEM simulation at the microscale; (iii) the surface topography acquired at time 1 after use.

The experimental surface topography map was depicted using the same color legend at times 0 and 1 for each microsurface for a more straightforward interpretation of the results. The comparison demonstrates that the computational tool allows, in most cases, a good prediction of the areas subjected to wear pattern formation consistent with the observation of the experimental replicas. In fact, the contact areas in the second column in Fig. 11 match the areas where the surface elevation is reduced due to tool usage, however we would like to remind that the overlap of the two T is not perfect in all areas. The use traces captured by the confocal acquisition in the valleys are not very well predicted by the BEM simulation, probably because the medium and the roughness of the active tool are not included in this digital twin model.

Moreover, the confocal microscope acquisitions pre- and post-use indicate that the microscale surfaces 5 and 8 have the major extent of use traces in line with the expected outcome of the average pressures computed from the BEM. Indeed, in the computational predictions, surfaces 5 and 8 are subject to the highest average contact pressure (around 71 and 76 MPa, respectively) and the highest percentage of real contact area, leading to the observed higher surface modifications.

4. Conclusion

It is important to note that multi-scale approaches have been increasingly applied to studying GSTs in recent traceological research. This is essential for accurately documenting and analyzing the diverse wear patterns that develop on these tools during their use. Traceologists have relied on integrating information obtained from different scales of analysis —ranging from macroscopic observations to microscopic

examinations— to construct a detailed understanding of tool use and the wear formation process. The multi-scale approach allows researchers to capture a comprehensive picture of the tool's surface. At the macroscopic level, researchers can observe overall tool morphology and wear patterns. In contrast, at the microscopic level, they can examine fine surface details such as micro-wear that provide insights into the specific task(s) performed with the tool.

Our pioneering study attempts not only to integrate information from different scales of analysis but also to integrate multi-scale and multi-technique data and exploit them in a computational tool to predict the area subject to use-related transformation. This integration involves photogrammetry and 3D model reconstruction to capture tool geometry and confocal profilometry to detail surface topography and measure roughness at a microscopic level. By constructing a cohesive dataset that combines data from both macro- and microscale, we aim to support a more comprehensive understanding of wear patterns and estimate the areas that underwent the most intense use-related transformation.

In this initial trial, we considered only the wear process occurring on the passive tool due to contact with a hypothetical flat surface of an active tool performing a vertical pounding action. At the current state, the computational model neglects the effect of having two rough surfaces in contact, considering only the roughness acquired on the passive tool. However, this aspect can be addressed in the future using the presented methodology but exploiting an "equivalent rough surface" computed from the two stones' rough surfaces in input. This equivalence is mathematically detailed in (Bemporad and Paggi, 2015). This operation requires studying carefully the alignment of the active tool use surface to the passive tool use surface at both scales. The presented manuscript represents only the first step for developing a more complex numerical model that requires a careful validation of each step before including all the factors affecting the real case study.

Moreover, the presence of the medium was neglected. With the aim of investigating the origin of the wear traces due to above and underground plant organs processing with GSTs (whose experimental data are available from replicated GSTs use in Sorrentino et al., 2023a), the formulation needs to be extended to consider third body contacts. Some suggestions to tackle this very complex problem can be found in the third medium contact (TMC) method (i.e., Frederiksen et al., 2024; Harish and Wriggers, 2019; Kruse et al., 2018), opening to new research perspectives.

Despite this limitation due to computational constraints, the results presented in this study are promising and show a good correspondence with the areas that underwent the most significant modifications in the experimental stone tool. The next step is to implement a more comprehensive model that overcomes the mentioned limitations by simulating contact with different mediums, adding the active tool roughness, and considering more types of gestures, including grinding. This will allow for various scenarios, facilitating an easier, more objective, and quicker comparison with archaeological records. More broadly, the BEM-based digital twin presented in this work represents an innovative strategy to localize and quantify use-wear in archaeological studies and gain new insights into those archeological research questions that involve contact between solids.

CRediT authorship contribution statement

Maria Rosaria Marulli: Writing – review & editing, Writing – original draft, Visualization, Validation, Software, Methodology, Formal analysis. **Giusi Sorrentino:** Writing – review & editing, Writing – original draft, Visualization, Validation, Software, Formal analysis, Data curation, Conceptualization. **Marco Paggi:** Writing – review & editing, Writing – original draft, Supervision, Software, Methodology, Conceptualization.

Declaration of competing interest

The authors declare that they have no known competing financial interests or personal relationships that could have appeared to influence the work reported in this paper.

Acknowledgements

The authors would like to thank Ivan Calandra for helpful discussions. MP and MRM would like to acknowledge the financial support of the Italian Ministry of University and Research (MUR) to the Project "Scientific computing for natural sciences, social sciences, and applications: methodological and technological development" (CUP D67G22000130001).

Appendix A. Supplementary data

Supplementary data to this article can be found online at https://doi.org/10.1016/j.jasrep.2024.104939.

Data availability

Data will be made available on request.

References

Adams, J.L., 2010. Understanding Grinding Technology through Experimentation. In: Ferguson, J.R. (Ed.), Designing Experimental Research in Archaeology, Examining Technology through Production and Use. University Press of Colorado, Boulder.

Adams J.L. (2002). Ground Stone Analysis: a technological approach. The University of Utah Press, pp. 336. ISBN: 0874807166.

Amidror, I., 2002. Scattered data interpolation methods for electronic imaging systems: a survey. J. Electron. Imaging 11, 157–176.

Astruc, L., Vargiolu, R., Zahouani, H., 2003. Wear assessments of prehistoric instruments. Wear 255, 341–347.

Barber, J.R., 2003. Bounds on the electrical resistance between contacting elastic rough bodies. Proc. r. Soc. London Ser. A 459, 53–66.

Bemporad, A., Paggi, M., 2015. Optimization algorithms for the solution of the frictionless normal contact between rough surfaces. Int. J. Solids Struct. 69, 94–105.

Bonari, J., Paggi, M., Dini, D., 2022. A new finite element paradigm to solve contact problems with roughness. Int. J. Solids Struct. 253, 111643.

Borri-Brunetto, C., Chiaia, B., Ciavarella, M., 2001. Incipient sliding of rough surfaces in contact: a multiscale numerical analysis. Comput. Methods in Appl. Mech. Eng. 190, 6053–6073.

Brown C.A., Hansen H.N., Jiang X.J, Blateyron F., Berglund J., Senin N., Bartkowiak T., Dixon, Le Goïc B.G., Quinsat Y., Stemp W.J., Thompson M.K., Ungar P.S., Zahouani E.H. (2018) Multiscale analyses and characterizations of surface topographies. CIRP Annals, 67(2), 839-862.

Calandra, I., 2022. A workflow for quality control in surface texture analysis applied to teeth and tools. J. Archaeol. Sci. Rep. 46, 103692.

Calandra, I., Gneisinger, W., Marreiros, J., 2020. A versatile mechanized setup for controlled experiments in archeology. Sci. Technol. Archaeol. Res. 6, 30–40.

Carpinteri, A., Paggi, M., 2005. Size-scale effects on the friction coefficient. Int. J. Solids Struct. 42, 2901–2910.

Ciavarella, M., 1998. Tangential loading of general three-dimensional contacts. ASME J. Appl. Mech. 64, 998–1003.

Doron H. (2024) https://www.mathworks.com/matlabcentral/fileexchange/6678-stlread, MATLAB Central File Exchange. Accessed on June 17, 2024.".

Dubreuil L., Savage D., Delgado-Raack S., Plisson H., Stephenson B., De La Torre I. (2015) Current analytical frameworks for studies of use– wear on ground stone tools. In: Use-wear and residue analysis in archaeology; João Manuel Marreiros, Juan F. Gibaja Bao, Nuno Ferreira Bicho, Eds. Springer Cham, pp. 105–158. Jäger J. (1998) A new principle in contact mechanics. ASME J. Trib. 120, 677-684.

Frederiksen, A.H., Rokoš, O., Poulios, K., Sigmund, O., Geers, M.G.D., 2024. Adding Friction to Third Medium Contact: A crystal plasticity inspired approach. Comput. Methods Appl. Mech. Eng. 432, 117412.

Harish, A.B., Wriggers, P., 2019. Modeling of two-body abrasive wear of filled elastomers as a contact-induced fracture process. Tribol. Int. 138, 16–31.

Hills D. A., Moore M. R. (2022) Partial slip problems in contact mechanics. In: Fretting Wear and Fretting Fatigue: Fundamental Principles and Applications, Elsevier, pp. 231-259, ISBN 9780128240960.

Jäger, J.A., 1998. New Principle in Contact Mechanics. J. Tribol. 120, 677–684.

Kruse, R., Nguyen-Thanh, N., Wriggers, P., De Lorenzis, L., 2018. Isogeometric frictionless contact analysis with the third medium method. Comput. Mech. 62, 1009–1021.

Liu, G., Wang, Q., Lin, C., 1999. A survey of current models for simulating the contact between rough surfaces. Tribol. Trans. 42 (3), 581–591.

Marreiros, J., Calandra, I., Gneisinger, W., Paixão, E., Pedergnana, A., Schunk, L., 2020. Rethinking Use-Wear Analysis and Experimentation as Applied to the Study of Past Hominin Tool Use. J. Paleolit. Archaeol. 3, 475–502.
Marulli, M.R., Bonari, J., Reinoso, J., Paggi, M., 2023a. A coupled approach to predict cone-cracks in spherical indentation tests with smooth or rough indenters. J. Mech. Phys. Solids 178, 105345.
Marulli, M.R., Sorrentino, G., Menna, F., Paggi, M., 2023b. Digital twin models of replicative ground stones: insight into simulating usage of Upper Paleolithic tools. Sci. Rep. 13 (1), 18298.
Müser, M.H., et al., 2017. Meeting the contact-mechanics challenge. Tribol. Lett. 65, 1–18.
Paggi, M., Pohrt, R., Popov, V.L., 2014. Partial-slip frictional response of rough surfaces. Sci. Rep. 4 (1), 5178.
Paixão, E., Pedergnana, A., Marreiros, J., Dubreuil, L., Prévost, M., Zaidner, Y., Carver, G., Gneisinger, W., 2021. Using mechanical experiments to study ground stone tool use: Exploring the formation of percussive and grinding wear traces on limestone tools. J. Archaeol. Sci, Rep, p. 37.
Paixão, E., Marreiros, J., Dubreuil, L., Gneisinger, W., Carver, G., Prévost, M., Zaidner, Y., 2022. The Middle Paleolithic ground stones tools of Nesher Ramla unit V (Southern Levant): A multi-scale use-wear approach for assessing the assemblage functional variability. Quat. Int. 624, 94–106.
Rausch, H., Marreiros, J., Kullmer, O., Schunk, L., Gneisinger, W., Calandra, I., 2024. An experimental approach on dynamic occlusal fingerprint analysis to simulate use-wear localisation and development on stone tools. Sci. Rep. 14, 1–11.
Rey, V., Anciaux, G., Molinari, J.F., 2017. Normal adhesive contact on rough surfaces: efficient algorithm for FFT-based BEM resolution. Comput. Mech. 60, 69–81.
Sorrentino, G., Longo, L., Obada, T., Borghi, A., Re, A., Paggi, M., Lo, G.A., 2023a. Tracing old gestures: A multiscale analysis of ground stone tools developed on sequential lab-controlled replicative experiments. Heritage 6 (6), 4737–4767.
Sorrentino, G., Menna, F., Remondino, F., Paggi, M., Longo, L., Borghi, A., Re, A., Lo, G. A., 2023b. Close-range photogrammetry reveals morphometric changes on replicative ground stones. PLoS One 18 (8), e0289807.
Sorrentino, G., Longo, L., Lo, G.A., Re, A., Paggi, M., 2024. Replicative experimental use of Palaeolithic Ground Stone Tools: Tracing and quantifying wear. J. Archaeol. Sci. Rep. 57, 104669.
Stemp, W.J., Stemp, M., 2001. UBM Laser Profilometry and Lithic Use-wear Analysis: A Variable Length Scale Investigation of Surface Topography. J. Archaeol. Sci. 28, 81–88.
Vakis, A.I., et al., 2018. Modeling and simulation in tribology across scales: An overview. Tribol. Int. 125, 169–199.